Sensitised near-infrared luminescence from lanthanide(III) centres using Re(I) and Pt(II) diimine complexes as energy donors in d–f dinuclear complexes based on 2,3-bis(2-pyridyl)pyrazine†

Frazer Kennedy,[a] Nail M. Shavaleev,[b] Thelma Koullourou,[c] Zoë R. Bell,[b] John C. Jeffery,[b] Stephen Faulkner*[c] and Michael D. Ward*[a]

Received 9th November 2006, Accepted 9th February 2007
First published as an Advance Article on the web 28th February 2007
DOI: 10.1039/b616423d

The luminescent transition metal complexes $[Re(CO)_3Cl(bppz)]$ and $[Pt(CC–C_6H_4CF_3)_2(bppz)]$ [bppz = 2,3-bis(2-pyridyl)pyrazine], in which one of the diimine binding sites of the potentially bridging ligand bppz is vacant, have been used as 'complex ligands' to make heterodinuclear d–f complexes by attachment of a $\{Ln(dik)_3\}$ fragment (dik = a 1,3-diketonate) at the vacant site. When Ln = Pr, Nd, Er or Yb the lanthanide centre has low-energy f–f excited states capable of accepting energy from the ^{3}MLCT excited state of the Pt(II) or Re(I) centre, quenching the ^{3}MLCT luminescence and affording sensitised lanthanide(III)-based luminescence in the near-IR region. UV/Vis and luminescence spectroscopic titrations allowed measurement of (i) the association constants for binding of the $\{Ln(dik)_3\}$ fragment at the vacant diimine site of $[Re(CO)_3Cl(bppz)]$ or $[Pt(CC–C_6H_4CF_3)_2(bppz)]$, and (ii) the degree of quenching of the ^{3}MLCT luminescence according to the nature of the Ln(III) centre. In all cases Nd(III) was found to be the most effective of the series at quenching the ^{3}MLCT luminescence of the d-block component because the high density of f–f excited states of the appropriate energy make it a particularly effective energy-acceptor.

Introduction

In the last few years there has been a lot of interest from many groups on the preparation and study of mixed-metal d–f assemblies in which a strongly light-absorbing transition-metal chromophore acts as an antenna group for sensitisation of luminescence from the lanthanide(III) fragment.[1–3] The use of d-block chromophores as antenna groups in this way overcomes the inherently low light absorption characteristics of lanthanide(III) ions, and a very large collection of d-block units is available which combine the desirable characteristics of chemical and photochemical stability, the availability of well-characterised long-lived excited states which can act as effective energy-donors, and strong absorption of light at more or less any desired wavelength. Generally, given the excited-state energies of the d-block chromophores used, near-infrared emissive lanthanides [Pr(III), Nd(III), Er(III), Yb(III)] have been used as the energy acceptors.

We have been following two quite distinct strategies for preparation of such d–f arrays. Crystallisation of luminescent cyanometallate complex anions such as $[Ru(bipy)(CN)_4]^{2-}$ with lanthanide cations affords a wide range of cyanide-bridged Ru(II)/Ln(III) coordination networks in which the luminescence of the $[Ru(bipy)(CN)_4]^{2-}$ units is quenched by the Ln(III) centre with concomitant appearance of sensitised near-infrared luminescence.[2] Alternatively, d-block complexes bearing a pendant peripheral diimine site can be used to form adducts with Ln(diketonate)$_3$ fragments in low-polarity solvents; again, excitation of the d-block component in the visible region generates sensitised Ln(III)-based near-infrared luminescence following d → f energy-transfer.[3]

The d → f energy-transfer process can be followed in two ways. Firstly, the appearance of sensitised Ln(III)-based luminescence is obvious evidence that energy-transfer has occurred; if a rise-time is detectable then the energy-transfer rate can be estimated. Usually this is not possible, because efficient d → f energy-transfer occurs on a timescale of nanoseconds and the detectors commonly used for measuring NIR luminescence lifetimes cannot resolve such short rise-times because of their long response time. We have observed rise-times for sensitised Ln(III)-based luminescence only when the energy-transfer process is relatively slow and a rise time of the order of 100 ns could be detected by deconvolution techniques.[2a] Alternatively, if the d-block energy-donor is luminescent, the degree of luminescence quenching—manifested in a reduction of the luminescence lifetime—provides quantitative information on energy-transfer.[2b,3d] This is technically much easier due to the availability of very fast, sensitive detectors in the visible region which allow residual luminescence lifetimes on the nanosecond scale to be measured easily.

In a recent paper we showed how luminescence from the complexes $[Re(bpym)(CO)_3Cl]$ and $[Pt(bpym)(CC–C_6H_4CF_3)_2]$ (bpym = 2,2′-bipyrimidine) was completely quenched on binding of various Ln(diketonate)$_3$ fragments (Ln = Nd, Er, Yb) to the vacant site of the bipyrimidine bridging ligand.[3c] The d → f

[a]*Department of Chemistry, University of Sheffield, Sheffield, UK S3 7HF. E-mail: m.d.ward@Sheffield.ac.uk*
[b]*School of Chemistry, University of Bristol, Cantock's Close, Bristol, UK BS8 1TS*
[c]*Department of Chemistry, University of Manchester, Oxford Road, Manchester, UK M13 9PL. E-mail: stephen.faulkner@manchester.ac.uk*

† Electronic supplementary information (ESI) available: Tables S1 and S2 and Fig. S1. See DOI: 10.1039/b616423d

energy-transfer in these systems was clearly fast compared to the limitations of the equipment, *i.e.* $> 10^9$ s^{-1}. In order to slow down the energy-transfer so that residual luminescence lifetimes can be determined, which will allow us to see which d/f combinations in an isostructural series are the best for achieving sensitised near-infrared luminescence, we have prepared a related series of complexes based on the longer bridging ligand 2,3-bis(2-pyridyl)pyrazine (bppz) (see Scheme 1). In this paper we describe the syntheses, structural and photophysical properties of this set of d-block complexes and their d/f adducts with a range of different Ln(diketonate)$_3$ fragments.

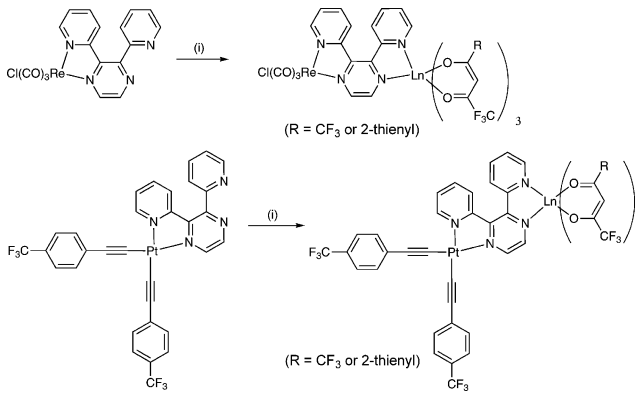

Scheme 1 (i) $Ln(dik)_3(H_2O)_2/CH_2Cl_2$.

Results and discussion

Syntheses and crystallography

The complex $[Re(CO)_3Cl(bppz)]$ has been prepared before,[4] we obtained crystals of the chloroform solvate from an NMR sample. The structure and geometry of the complex molecule (Fig. 1, Table 1) contain no surprises, with the metric parameters of the pseudo-octahedral Re(I) centre being typical for complexes of this type. The coordinated diimine unit is not planar, with the coordinated pyridyl ring containing N(11) being twisted from the mean plane of the pyrazine ring by 18°, in order to avoid steric interference with the pendant pyridyl ring [containing N(31)] which is twisted from the mean plane of the pyrazine ring by 44°. This conformation of a mono-coordinated bppz ligand is typical.[4b]

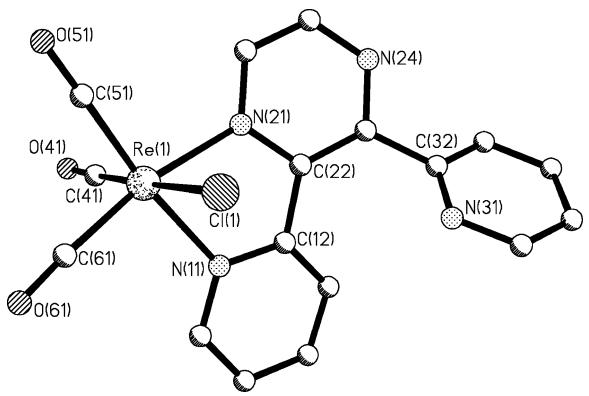

Fig. 1 Molecular structure of the metal complex unit of $[Re(CO)_3Cl(bppz)]\cdot CHCl_3$.

Table 1 Selected bond distances (Å) and angles (°) for the structure of $[Re(CO)_3Cl(bppz)]\cdot CHCl_3$

Re(1)–C(51)	1.920(6)	Re(1)–N(21)	2.161(4)
Re(1)–C(61)	1.932(6)	Re(1)–N(11)	2.171(5)
Re(1)–C(41)	2.006(6)	Re(1)–Cl(1)	2.4592(16)
C(51)–Re(1)–C(61)	90.8(2)	C(41)–Re(1)–N(11)	92.0(2)
C(51)–Re(1)–C(41)	88.7(2)	N(21)–Re(1)–N(11)	74.38(17)
C(61)–Re(1)–C(41)	92.4(2)	C(51)–Re(1)–Cl(1)	92.83(19)
C(51)–Re(1)–N(21)	98.5(2)	C(61)–Re(1)–Cl(1)	90.93(18)
C(61)–Re(1)–N(21)	169.0(2)	C(41)–Re(1)–Cl(1)	176.33(15)
C(41)–Re(1)–N(21)	93.72(19)	N(21)–Re(1)–Cl(1)	82.75(13)
C(51)–Re(1)–N(11)	172.9(2)	N(11)–Re(1)–Cl(1)	86.11(13)
C(61)–Re(1)–N(11)	96.2(2)		

The complex $[Pt(CC–C_6H_4CF_3)_2(bppz)]$ is a new member of the series of Pt(II)–diimine-diacetylide complexes which have attracted considerable attention recently for their luminescence properties,[5] the trifluoromethyl substituents on the phenylacetylide ligands enhance the ^{3}MLCT energy and lifetime.[3c,5c] It was prepared in 64% yield from the known complex $[Pt(bppz)Cl_2]$[6] by cross-coupling with $F_3C–C_6H_4$-CCH in the usual way.[5] We could not obtain X-ray quality crystals of it, but we did get crystals of the non-fluorinated analogue $[Pt(CC–C_6H_4CH_3)_2(bppz)]$ which was prepared using the same method. The structure and metric parameters are in Fig. 2 and Table 2. The Pt(II) centre has the usual nearly square-planar geometry, with the mono-coordinated bppz ligand having a similar conformation to that observed for $[Re(CO)_3Cl(bppz)]$; thus the pyridyl ring containing N(11) twisted away from the plane of the adjacent pyrazine ring by 14°, whereas the pendant pyridyl ring

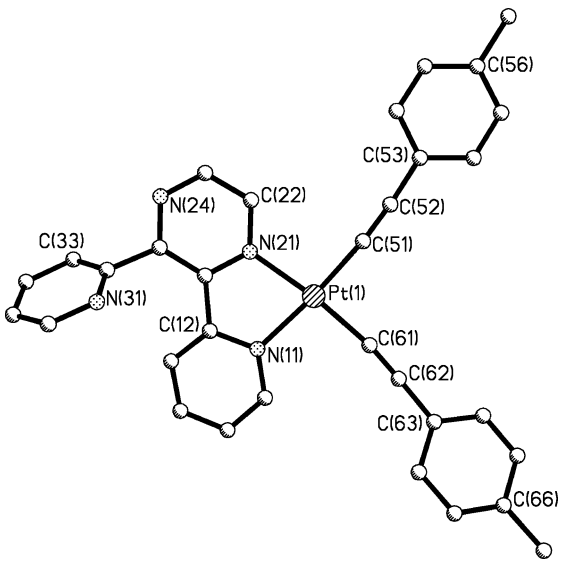

Fig. 2 Molecular structure of $[Pt(CC–C_6H_4CH_3)_2(bppz)]$.

Table 2 Selected bond distances (Å) and angles (°) for the structure of $[Pt(CC–C_6H_4CH_3)_2$ (bppz)]

Pt(1)–C(51)	1.948(7)	Pt(1)–N(21)	2.061(6)
Pt(1)–C(61)	1.959(7)	C(51)–C(52)	1.204(9)
Pt(1)–N(11)	2.053(5)	C(61)–C(62)	1.170(10)
C(51)–Pt(1)–C(61)	89.3(3)	C(51)–Pt(1)–N(21)	96.9(2)
C(51)–Pt(1)–N(11)	174.5(3)	C(61)–Pt(1)–N(21)	173.1(2)
C(61)–Pt(1)–N(11)	95.8(2)	N(11)–Pt(1)–N(21)	78.1(2)

containing N(31) is twisted out of the plane of the pyrazine ring by 60°. The molecules are stacked such that the planar central Pt(diimine) portions of the structures overlap, but they are offset such that there are no short Pt · · · Pt contacts.

Adducts of these complexes $[Cl(CO)_3Re(\mu\text{–}bppz)Ln(hfac)_3]$ (hereafter, **Re-Ln**) or $[Cl(CO)_3Re(\mu\text{–}bppz)Ln(tta)_3]$ (hereafter, **Re-Ln′**) were simply prepared by mixing a 1 : 1 molar ratio of $[Re(CO)_3Cl(bppz)]$ and the appropriate $Ln(diketonate)_3(H_2O)_2$ in a CH_2Cl_2/hexane mixture and allowing the solution to evaporate. For the series **Re-Ln′**, containing the diketonate ligand tta (anion of thenoyl-trifluoro-acetylacetonate) X-ray quality crystals were obtained for Ln = Gd (the analogue with Ln = Nd was described in an earlier communication).[7] The structure and metric parameters of **Re-Gd′** are in Fig. 3 and Table 3. The fact that both diimine sites are now coordinated to metal ions results in a more symmetrical arrangement of the bridging ligand, with the pyridyl rings coordinated to Re(1) and Gd(1) being twisted out of the plane of the central pyrazine ring by 22° and 37°, respectively. Gd(1) is in an N_2O_6 8-coordinate environment, from the three diketonate ligands and one diimine donor, the coordination geometry is approximately square antiprismatic, with O(51)/O(54)/O(61)/O(64) forming one square plane and N(11)/N(21)/O(41)/O(44) forming the other. The Re · · · Gd separation across the bridging ligand is 7.40 Å, *cf.* separations of *ca.* 6.3 Å in related complexes with bpym as bridging ligand.[3e] Adducts of $[Pt(CC\text{–}C_6H_4CF_3)_2(bppz)]$ with $Ln(diketonate)_3$ units also clearly formed in CH_2Cl_2 solution, on the basis the colour change in the Pt(II) chromophore associated with Ln(III) binding at the other site of bppz (see Fig. 4), but none afforded X-ray quality crystals.

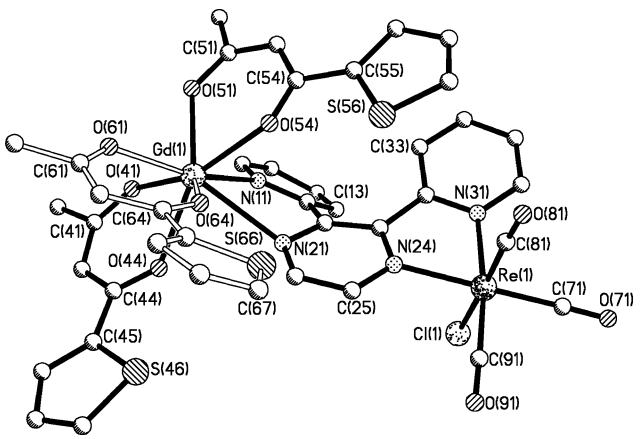

Fig. 3 Molecular structure of $[Cl(CO)_3Re(\mu\text{-}bppz)Gd(tta)_3]$ (F atoms of the tta ligands omitted for clarity, one of the tta ligands is shown with hollow bonds for clarity).

Table 3 Selected bond distances (Å) and angles (°) for the structure of $[Cl(CO)_3Re(\mu\text{–}bppz)Gd(tta)_3]$

Gd(1)–O(61)	2.306(3)	Re(1)–C(91)	1.916(5)
Gd(1)–O(44)	2.345(3)	Re(1)–C(71)	1.920(5)
Gd(1)–O(54)	2.347(3)	Re(1)–C(81)	1.932(5)
Gd(1)–O(41)	2.357(3)	Re(1)–N(31)	2.162(4)
Gd(1)–O(64)	2.377(3)	Re(1)–N(24)	2.171(3)
Gd(1)–O(51)	2.386(3)	Re(1)–Cl(1)	2.4620(15)
Gd(1)–N(11)	2.564(4)		
Gd(1)–N(21)	2.674(3)		
C(91)–Re(1)–C(71)	87.6(2)	C(81)–Re(1)–N(24)	96.04(16)
C(91)–Re(1)–C(81)	91.5(2)	N(31)–Re(1)–N(24)	74.55(13)
C(71)–Re(1)–C(81)	91.5(2)	C(91)–Re(1)–Cl(1)	93.08(17)
C(91)–Re(1)–N(31)	172.62(17)	C(71)–Re(1)–Cl(1)	89.24(15)
C(71)–Re(1)–N(31)	99.09(17)	C(81)–Re(1)–Cl(1)	175.41(15)
C(81)–Re(1)–N(31)	91.54(17)	N(31)–Re(1)–Cl(1)	83.88(10)
C(91)–Re(1)–N(24)	98.43(17)	N(24)–Re(1)–Cl(1)	82.79(10)
C(71)–Re(1)–N(24)	170.25(17)		

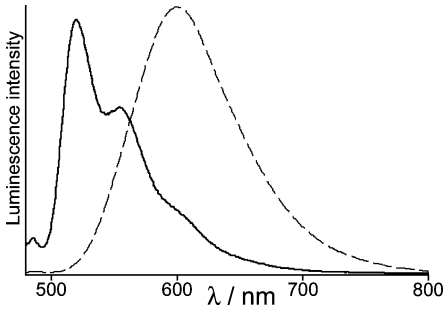

Fig. 4 Normalised luminescence spectra of $[Pt(CC\text{–}C_6H_4CF_3)_2(bppz)]$, (a) at 77 K in a 2-Me-thf glass (solid line) and (b) at room temperature in CH_2Cl_2 solution.

We also prepared the known related complex $[Re(CO)_3Cl(dpq)]$ [dpq = 2,3-bis(2-pyridyl)quinoxaline][8] to see if $Ln(diketonate)_3$ adducts could be formed, however this was less successful, with the only crystalline product obtained, $[Re(CO)_3Cl(dpq)][Gd(hfac)_3(H_2O)_2]\cdot C_6H_6$, showing that the two components $[Re(CO)_3Cl(dpq)]$ and $[Gd(hfac)_3(H_2O)_2]$ are not associated in the solid state but have co-crystallised. Although it is not what we had hoped for it is not without interest and the details are included as ESI.† In view of the relatively weak association of $Ln(diketonate)_3$ fragments to the vacant binding site of $[Re(CO)_3Cl(dpq)]$ we did not investigate this system further, but confined our solution luminescence studies to the $[Cl(CO)_3Re(\mu\text{-}bppz)Ln(hfac)_3]$ (**Re-Ln**), $[(CF_3C_6H_4CC)_2Pt(\mu\text{-}bppz)Ln(hfac)_3]$ (**Pt-Ln**) and $[(CF_3C_6H_4CC)_2Pt(\mu\text{-}bppz)Ln(tta)_3]$ (**Pt-Ln′**) series.

Solution photophysical studies

(i) Studies of Re-based and Pt-based luminescence quenching: d → f energy-transfer rates. The ^{1}MLCT absorption maximum of $[Re(CO)_3Cl(bppz)]$ is at *ca.* 400 nm (depending on the solvent) and its luminescence emission maximum was reported to be at 670 nm in MeCN.[4a,4c] We found the luminescence in aerated CH_2Cl_2 solution to be centred at 665 nm with $\tau = 13$ ns, and we also found that the unstructured luminescence maximum at 77 K (2-Me-thf glass) is at 575 nm, giving a ^{3}MLCT energy of 17 400 cm^{-1}. $[Pt(CC\text{–}C_6H_4CF_3)_2(bppz)]$ is much more strongly luminescent; in aerated CH_2Cl_2 solution its ^{1}MLCT absorption band is at 420 nm, and its luminescence maximum is at 600 nm with $\tau = 250$ ns. At 77 K (2-Me-thf glass) a structured luminescence profile (Fig. 4) is seen with the lowest-energy maximum at 520 nm, giving a ^{3}MLCT energy of 19 200 cm^{-1}.

We could observe the effect of a $Ln(diketonate)_3$ fragment binding to the vacant site of each of these by carrying out UV/Vis and luminescence titrations, adding small portions of $Ln(hfac)_3(H_2O)_2$ to solutions of the d-block complex in CH_2Cl_2. The results obtained with $[Pt(CC\text{–}C_6H_4CF_3)_2(bppz)]$ are in Fig. 5. As the $\{Ln(hfac)_3\}$ fragment associates, the ^{1}MLCT transition of the Pt(II) complex is red-shifted from 425 nm to 450 nm

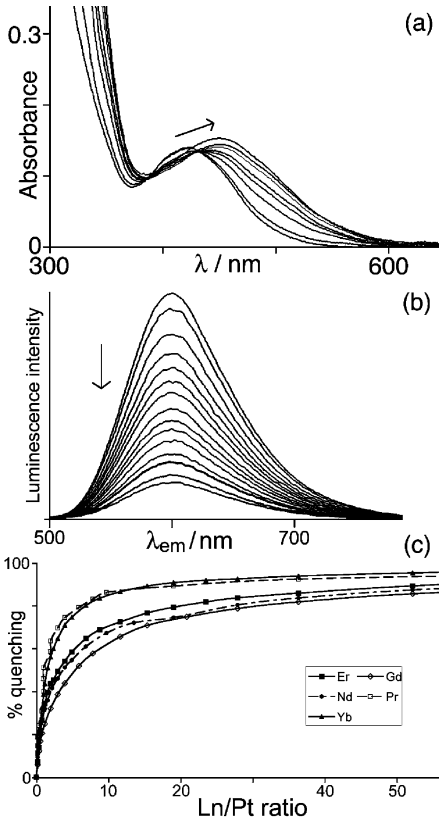

Fig. 5 Effects on (a) absorption and (b) luminescence spectra of $[Pt(CC–C_6H_4CH_3)_2(bppz)]$ (2×10^{-5} M) on titration with $[Yb(hfac)_3(H_2O)_2]$ in CH_2Cl_2 solution. Part (c) shows the extent of quenching of the luminescence intensity of $[Pt(CC–C_6H_4CH_3)_2(bppz)]$ *vs.* the amount of added $[Ln(hfac)_3(H_2O)_2]$ for a range of Ln, these data were used to calculate the 1 : 1 association constants associated with eqn (1) (see main text and Table 5).

(which causes a deepening of the colour), and the luminescence is quenched to an extent depending on the identity of the Ln centre. The luminescence quenching is manifested in both a reduction in luminescence intensity (Fig. 5), and also the appearance of a short-lived component in the time-resolved measurements. As more of the $Ln(hfac)_3(H_2O)_2$ is added to a fixed amount of $[Pt(CC–C_6H_4CF_3)_2(bppz)]$ during the titration, the luminescence decay shows both a long-lived component characteristic of residual free $[Pt(CC–C_6H_4CF_3)_2(bppz)]$ and a short-lived component characteristic of the adduct **Pt-Ln**. The long lived component becomes less significant and the short-lived component dominates as the titration proceeds, because of the equilibrium shown in eqn (1) (where '**M**–NN' denotes a metal complex ligand with a vacant diimine site, and 'dik' denotes a diketonate).

$$\mathbf{M}\text{–NN} + Ln(dik)_3(H_2O)_2 = \mathbf{M}\text{–NN–}Ln(dik)_3 + 2H_2O \qquad (1)$$

The red-shift of the absorption maximum during the titration is a consequence of the bppz LUMO being reduced in energy on coordination of an electropositive Ln(III) centre. It might be expected that this would also result in a reduction in the ^{3}MLCT energy and luminescence lifetime, following the energy-gap law.[9] The effects of this can be seen by using Ln(III) centres which cannot quench the excited state by energy-transfer, either because the Ln(III) concerned has only very high-energy f–f excited states [Gd(III), whose lowest energy excited state is at $\approx 32\,000$ cm^{-1}] or has no f–f excited states at all [La(III), $4f^0$; Lu(III), $4f^{14}$].

Rather surprisingly, titration of $[Pt(CC–C_6H_4CF_3)_2(bppz)]$ with $Gd(hfac)_3(H_2O)_2$ resulted in a very substantial degree of quenching of the Pt(II)–based luminescence intensity [*cf.* Fig. 5(b)] with the lifetimes being reduced from 250 ns to 18 (±1) ns. This has occurred despite there being no significant red-shift in the emission maximum of the **Pt–Gd** adduct compared to free $[Pt(CC–C_6H_4CF_3)_2(bppz)]$; thus, although the ^{1}MLCT absorption maximum is red-shifted by *ca.* 1300 cm^{-1} the corresponding ^{3}MLCT emission maximum is scarcely affected so the effects of the energy-gap law will not be significant in reducing the luminescence. This quenching must therefore be ascribed to an alteration in the vibrational behaviour of the complex when the $Ln(dik)_3$ fragment binds which facilitates non-radiative deactivation. To confirm that this is a mechanical effect and not related to the specific electron configuration or paramagnetism of Gd(III) ($4f^7$), we performed the same experiment using diamagnetic $Lu(hfac)_3(H_2O)_2$ and achieved an essentially identical result, with >90% quenching of luminescence intensity and reduction in the residual Pt-based luminescence lifetime to 17 (±1) ns. Fitting the luminescence intensities during these titrations to a 1 : 1 binding isotherm allows determination of the association constant of the equilibrium in eqn (1) as 4.6×10^4 M^{-1} for Gd(III) and 9.6×10^4 M^{-1} for Lu(III), with the smaller (and hence more Lewis-acidic) Lu(III) ion giving the higher association constant.

Comparable titrations with other $Ln(hfac)_3(H_2O)_2$ species [Ln = Pr, Nd, Er, Yb, see Fig. 5], which have low-energy f–f levels capable of quenching the Pt(II)-based ^{3}MLCT state, result in similar changes in the UV/Vis and luminescence data, with the exception that the luminescence quenching goes nearer to completion because of the additional effects of d → f energy-transfer. In each case we could measure the residual lifetime of the Pt(II)-based luminescence at the end of the titration, and also determine an association constant (*cf.* eqn (1)). The data are summarised in Table 4. Looking first at the association constants, there is a general increase by approximately a factor of two from the least to the most Lewis-acidic Ln(III) ion, although the variation is not smooth. Secondly, the degree of quenching of the Pt(II)-based luminescence, as shown by the luminescence lifetime of the **Pt-Ln** adduct at the end of the titration, varies between different lanthanides. The shortest residual lifetime for Pt(II)-based luminescence occurs in **Pt-Nd** ($\tau \approx 1$ ns); on the basis of eqn (2), where τ_q is the 'quenched' lifetime (*i.e.* 1 ns) and τ_u is the

Table 4 Summary of stability constant data and Pt(II)-based ^{3}MLCT luminescence data for the series **Pt-Ln**, **Pt-Ln′** and **Re-Ln**

	Pt–Ln series		Pt–Ln′ series		Re–Ln series	
	τ/ns[a]	K/M^{-1}	τ/ns[a]	K/M^{-1}	τ/ns[a]	K/M^{-1}
Pr	3	4.8×10^4	7	9.0×10^3	2	1.3×10^5
Nd	1	5.6×10^4	1	1.5×10^4	2	4.1×10^4
Gd	18	4.6×10^4	70	2.1×10^4	3	2.5×10^4
Er	2	8.6×10^4	4	2.2×10^4	2	2.8×10^5
Yb	2	1.9×10^5	6	7.0×10^3	2	2.4×10^5
Lu	17	9.6×10^4	—[b]	—[b]	2	2.3×10^4

[a] Detector response function, 0.5 ns, values are therefore quoted to the nearest nanosecond. [b] Not measured.

'unquenched' lifetime taken from either the **Pt-Gd** adducts (*i.e.* 18 ns) or the **Pt-Lu** adduct (*i.e.* 17 ns) in the absence of energy-transfer effects, the Pt → Nd energy-transfer rate k_{EnT} is $\approx 10^9$ s^{-1}.

$$k_{EnT} = 1/\tau_q - 1/\tau_u \quad (2)$$

For the other lanthanides the residual Pt(II)-based lifetime is a little longer, between 2 and 3 ns, implying a slightly slower value for k_{EnT} with the smallest value being $\approx 3 \times 10^8$ s^{-1} for Pt → Pr energy-transfer. All of these residual lifetimes τ_q are close to the limit of what can be measured accurately with our instrument (whose instrument response function is *ca.* 0.5 ns) but the factor of 3 difference between the shortest and the longest—1 ns, for **Pt-Nd**, *vs.* 3 ns, for **Pt-Pr**—is significant and implies that Nd(III) is the most effective quencher of the Pt(II) chromphore. The reasons for this are discussed later.

Use of the complexes $Ln(tta)_3(H_2O)_2$ to generate the series of adducts **Pt-Ln′** (with Ln = Pr, Nd, Gd, Er, Yb) gave comparable results with some important similarities and some minor differences. As before, addition of the $\{Ln(tta)_3\}$ fragment to the secondary binding site of $[Pt(CC–C_6H_4CF_3)_2(bppz)]$ results in a red-shift of the Pt(II)-based ^{1}MLCT absorption and quenching of the ^{3}MLCT luminescence, and from the luminescence intensity data recorded during the titration the 1 : 1 association constants could be determined. These are significantly smaller than for the **Pt-Ln** series, by on average one order of magnitude. This may be ascribed to either (i) the greater bulk of the tta ligands compared to hfac, which slightly hinders formation of the 8-coordinate adducts, and/or (ii) the higher electron-withdrawing effect of the hfac ligands (each with six F atom substituents) which will increase slightly the partial positive charge on the Ln(III) centre and thereby result in slightly stronger electrostatic bonding for the hfac series **Pt-Ln** compared to the tta series **Pt-Ln′**. Also we found that the variation in binding constants throughout the **Pt-Ln′** series no longer correlates with the size of the Ln(III) ion, in fact Yb(III) gives the weakest binding to $[Pt(CC–C_6H_4CF_3)_2(bppz)]$, possibly because the combination of bulkier tta ligands and the smaller ionic radius results in a higher degree of steric crowding in the 8-coordinate adduct which overcomes the expected slight increase in electrostatic metal/ligand interactions.

The luminescence lifetimes in this series, however, clearly show the same general behaviour as observed in the **Pt-Ln** series. The adduct **Pt-Gd′** shows the lowest degree of quenching of the Pt(II) ^{3}MLCT luminescence because of the absence of any energy-transfer component, with the residual lifetime τ_u of 70 ns. The other energy-accepting lanthanides have a much greater quenching effect, with (again) Nd(III) causing the highest degree of quenching ($\tau_q \approx 1$ ns) and Pr(III) causing the least ($\tau_q = 7$ ns). Thus, on the basis of eqn (2), the Pt → Ln energy-transfer rates in this series vary from $\approx 10^9$ s^{-1} (for Ln = Nd) to 1.4×10^8 s^{-1} (for Ln = Pr).

The variation in Pt → Ln energy-transfer rates in both series may be accounted for by considering the availability of f–f excited states on the Ln(III) acceptor which are capable of acting as energy acceptors. For energy-transfer to occur from the ^{3}MLCT state of $[Pt(CC–C_6H_4CF_3)_2(bppz)]$ to the Ln(III) centre there must be f–f excited levels available which are at least 2000 cm^{-1} below the ^{3}MLCT level, but not so far below that there is no overlap with the ^{3}MLCT emission spectrum. The gradient of > 2000 cm^{-1} for d → f energy-transfer is necessary to prevent thermally-activated back energy-transfer from Ln(III) to the d-block component, *i.e.* without this gradient the d → f energy-transfer will be inefficient at room temperature.[10] Nd(III) has a particularly high density of f–f excited states of appropriate energy (between *ca.* 11 000 and 16 000 cm^{-1}) which overlap well with the luminescence from $[Pt(CC–C_6H_4CF_3)_2(bppz)]$, and both we[3d] and others[1] have observed that Nd(III) is for this reason a particularly effective quencher of luminescence for d-block chromophores which luminesce in the 600–700 nm region in fluid solution. Pr(III), Yb(III) and Er(III) all have fewer f–f states in the relevant region and energy-transfer to them is accordingly slower. In the **Pt-Ln′** series the least effective energy-acceptors are Pr(III) and Yb(III), which is a consequence of the energy-accepting f–f level being low in energy [$^1G_4$ for Pr(III) and $^2F_{5/2}$ for Yb(III), both at $\approx$ 10 000 cm^{-1}] with concomitantly poor spectroscopic overlap with the emission spectrum of the Pt(II) donor unit. The relatively slow energy-transfer to Pr(III)—the slowest in the series—implies that the next highest energy level of Pr(III), $^1D_2$ at $\approx 17\,000$ cm^{-1}, is just too high in energy to be efficiently populated at room temperature by the ^{3}MLCT state of $[Pt(CC–C_6H_4CF_3)_2(bppz)]$ following the arguments given earlier.

Measurements of UV/Vis and luminescence spectra during the titration of $[Re(CO)_3Cl(bppz)]$ with $Ln(hfac)_3(H_2O)_2$ to generate the **Re-Ln** series in CH_2Cl_2 solution (Ln = Pr, Nd, Gd, Er, Yb) showed that, as with the **Pt-Ln** series, the association constants for adduct formation are *ca.* 10^5 M^{-1}. During the titration the stabilisation of the bppz LUMO results in a red-shift of the Re(I)-centred MLCT absorption from 414 nm to 450 nm, and also in progressive quenching of the luminescence band at 670 nm. In this series the **Re-Gd** adduct (in which there is no d → f energy-transfer) is nearly quenched to start with ($\tau_q = 3$ ns), presumably because of the introduction of additional vibrational deactivation pathways; the additional effects of energy-transfer with the other $\{Ln(hfac)_3\}$ fragments make relatively little difference, giving $\tau_q \approx$ 2 ns in every case. The values of τ_q for Ln = Pr, Nd, Er, Yb are sufficiently similar that no analysis of the relative Re → Ln energy-transfer rates in this series is possible. However, as with the two series **Pt-Ln** and **Pt-Ln′**, the occurrence of d → f energy-transfer is apparent from the appearance of sensitised luminescence from the Ln(III) centre in each case.

(ii) Studies on sensitised near-infrared luminescence from Nd(III), Er(III) and Yb(III). We could demonstrate in these series of adducts that d → f energy-transfer is occurring, not just from the quenching of the d-block component (previous section) but from the appearance of sensitised luminescence from the Ln(III) centre in many cases. The adducts were prepared *in situ* by combining $[Re(CO)_3Cl(bppz)]$ or $[Pt(CC–C_6H_4CF_3)_2(bppz)]$ with a five-fold excess of the appropriate $Ln(diketonate)_3(H_2O)_2$ species at a concentration sufficiently high to ensure a substantial degree of association based on the known association constants from Table 4. Although association may not be complete (*cf.* eqn (1)), by selective excitation of the d-block chromophore at >400 nm (where the Ln-diketonates do not absorb) and monitoring only sensitised Ln(III)-based luminescence in the near-IR region, only the associated d–f adducts were being interrogated. In this way we could see the characteristic luminescence of Yb(III) ($^2F_{5/2} \rightarrow {}^2F_{7/2}$ at 980 nm), Nd(III) ($^4F_{3/2} \rightarrow {}^4I_{11/2}$ at 1060 nm), Pr(III) ($^1D_2 \rightarrow {}^3F_4$ at 1030 nm) and Er(III) ($^4I_{13/2} \rightarrow {}^4I_{15/2}$ at 1530 nm) in the series **Re-Ln** and **Pt-Ln** (Table 5). The Er(III)–based luminescence

Table 5 Lifetimes of sensitised Ln(III)-based luminescence measured in CH_2Cl_2 solution using excitation at 430 nm into the Re(I)-based or Pt(II)-based MLCT absorptions

Complex	τ/μs
Re-Nd	0.2[a]
Pt-Nd	0.2[a]
Re-Yb	9.0[b]
Pt-Yb	7.4[b]
Pt-Pr	0.2[c]

[a] Measured at 1060 nm, estimated error ± 0.05 μs. [b] Measured at 980 nm, estimated error ± 0.2 μs. [c] Measured at 1030 nm, estimated error ± 0.05 μs.

was very weak and reliable lifetime values could not be obtained, however the characteristic luminescence, which could only arise from d → f energy-transfer, was present.

For the Yb(III) and Nd(III) adducts in each series, however, time-resolved measurements were possible. For **Re-Yb** and **Pt-Yb** the Yb(III)–based luminescence lifetimes from the $Yb(hfac)_3(NN)$ centres were 9 and 7.4 μs, respectively; for **Re-Nd** and **Pt-Nd** the sensitised Nd(III)–based luminescence lifetimes were likewise similar to one another at about 0.2 μs each. These are fairly typical values for such $Ln(diketonate)_3(NN)$ luminophores in aprotic, non-coordinating solvents, with the much lower values for Nd(III) arising from the presence of low-energy f–f states which are particularly easily quenched by overtones of C–H oscillators in either the solvent or the ligand set.[3] For **Pt-Pr** we could observe weak sensitised Pr(III)-based luminescence with a lifetime of *ca.* 0.2 μs; however, for **Re-Pr** the Pr(III)-based luminescence was almost non-existent, probably because the much shorter lifetime of the Re(I)-based ^{3}MLCT state compared to the Pt(II)-based ^{3}MLCT state means that Re → Pr energy-transfer is not fast enough to compete effectively with other deactivation pathways.

Conclusions

The luminescent complexes $[Re(CO)_3Cl(bppz)]$ and $[Pt(CC–C_6H_4CF_3)_2(bppz)]$, which both have a vacant diimine binding site, form d–f dinuclear adducts in which $\{Ln(diketonate)_3\}$ fragments bind at the secondary diimine site; association constants are in the range 10^4 M^{-1}–10^5 M^{-1} in CH_2Cl_2 solution. Compared to the analogous bipyrimidine-bridged d–f dinuclear complexes that we described recently[3c] the use of bppz as bridging ligand provides two advantages: (i) it is a better base, so association constants for $\{Ln(diketonate)_3\}$ binding are higher; (ii) the greater d–f separation slows down d → f energy-transfer to the extent that it can be quantified for different Ln(III) species by measuring the differential degrees of quenching of the d-block luminescence. In the Pt/Ln series in particular the rates of Pt → Ln energy-transfer vary over nearly an order of magnitude with Pr(III) and Yb(III) being less effective energy-acceptors than Nd(III). The d → f energy-transfer generates sensitised near-infrared luminescence from the Ln(III) ions.

Experimental

General details

Organic reagents and metal salts were purchased from Sigma-Aldrich and used as received. $[Re(CO)_3Cl(bppz)]$,[4] $[Pt(bppz)Cl_2]$,[6] $[Re(CO)_3Cl(dpq)]$[11] and $Ln(dik)_3·2H_2O$[12] were prepared according to the literature methods. Mass spectra (EI and FAB) were recorded on a VG-Autospec instrument. UV/Vis absorption spectra were recorded on a Cary 50 spectrometer using CH_2Cl_2 solutions. Steady-state luminescence spectra were recorded in aerated CH_2Cl_2 solutions, diluted to give an absorbance of 0.2 or less at the excitation wavelength, on a Perkin-Elmer LS-50 luminescence spectrometer. Luminescence lifetimes of the d-block complexes were acquired on an Edinburgh Instruments 'Mini-τ' instrument operating under single photon counting conditions, equipped with an EPL-405 picosecond pulsed diode laser (410 nm) as excitation source and a Hamamatsu R-928 photomultiplier detector. Wavelength selection for lifetime measurements was *via* the use of a band-pass filter. Instrumentation used to measure time-resolved emission spectra from lanthanides in the near-IR region has been described in a previous paper;[13] selective excitation at 430 nm of the Re(I)-based or Pt(II)-based ^{1}MLCT absorptions was achieved using a dye laser which was in turn pumped by an N_2 laser, as described previously.[13] Calculations of association constants from UV/Vis spectroscopic titration data were performed with the programs *NMRTit-HG* (for 1 : 1 complexes) kindly provided by Prof. C. A. Hunter of the University of Sheffield.[14]

Syntheses

$[Pt(CC-C_6H_4CF_3)_2(bppz)]$: A mixture of $Pt(bppz)Cl_2$ (1.97 g, 3.9 mmol), $i$$Pr_2NH$ (5 cm^3, 35.4 mmol) and anhydrous CuI (40 mg, catalyst) in freshly distilled CH_2Cl_2 (70 cm^3) under N_2 was stirred for 10 min, followed by the addition of 4-ethynyl-α,α,α-trifluorotoluene (2 cm^3, 12.3 mmol). The suspension was stirred under N_2 at room temperature for 24 h. After this time, the resultant dark red suspension was evaporated to dryness to remove traces of $i$$Pr_2NH$ and purified by column chromatography on silica eluting with MeOH–CH_2Cl_2 (1 : 100 to 5 : 95). The orange coloured fraction containing the product was reduced in volume and hexane added to precipitate the product. Yield: 64%. Anal. Calc. for $C_{32}H_{18}F_6N_4Pt$: C, 50.1; H, 2.4; N, 7.3. Found: C, 49.9; H, 2.2; N, 7.1%. ESMS: m/z 768 (M^+). UV VIS (CH_2Cl_2): nm (ε) 423 (7100), 287 (53 000).

$[Pt(CC-C_6H_4CH_3)_2(bppz)]$ was prepared and purified in an exactly similar way. Yield: 67%. Anal. Calc. for $C_{32}H_{24}N_4Pt$: C, 58.3; H, 3.7; N, 8.5. Found: C, 58.3; H, 3.7; N, 8.6%. FAB MS: m/z 682 (16%, $\{M + Na\}^+$), 660 (60%, M^+). UV VIS (CH_2Cl_2): nm (ε) 438 (7000), 271 (48 000). X-Ray quality crystals were grown by evaporation of a CH_2Cl_2 solution of the compound.

The adduct $[Cl(CO)_3Re(\mu\text{-}bppz)Ln(tta)_3]$ (**Re-Gd′**) was prepared for X-ray structural determination by slow partial evaporation of mixed CH_2Cl_2–hexane solution (1 : 1 v/v, initial volume approx. 25 ml) containing $Re(bppz)(CO)_3Cl$ and $Gd(TTA)_3·2H_2O$ in a 1 : 1 molar ratio. In 3–5 days orange needle-like crystals of the complexes were formed. Anal. Calcd. for $GdReC_{41}O_9ClN_4H_{22}S_3F_9$: C, 36.2; H, 1.6; N, 4.1. Found: C, 36.4; H, 1.4; N, 4.2%. IR (CH_2Cl_2), cm^{-1}: 2028, 1932, 1908. The remaining adducts were generated directly in solution for spectroscopic and luminescence studies by combining $[Pt(CC–C_6H_4CF_3)_2(bppz)]$ or $[Re(CO)_3Cl(bppz)]$ with the appropriate $Ln(dik)_3·2H_2O$ in dry CH_2Cl_2 (see main text).

Table 6 Crystallographic data for the crystal structures[a]

Complex	$[Re(CO)_3Cl(bppz)]\cdot CHCl_3$	$[Pt(CC–C_6H_4CH_3)_2(bppz)]$	$[Cl(CO)_3Re(\mu\text{-}bppz)\,Gd(tta)_3]$
Formula	$C_{18}H_{11}Cl_4N_4O_3Re$	$C_{32}H_{24}N_4Pt$	$C_{41}H_{22}ClF_9GdN_4O_9ReS_3$
Formula weight	659.31	659.64	1360.71
T/K	173(2)	173(2)	100(2)
Crystal system, space group	Monoclinic, $P2(1)/c$	Monoclinic, $P2(1)/c$	Monoclinic, $P2(1)/c$
a/Å	6.4657(16)	9.3819(16)	8.849(4)
b/Å	19.437(5)	19.480(4)	38.843(11)
c/Å	17.053(4)	14.6718(16)	13.404(5)
α/°	90	90	90
β/°	94.969(5)	90.031(19)	101.26(4)
γ/°	90	90	90
V/Å^3	2135.0(9)	2681.4(8)	4519(3)
Z	4	4	4
D_{calc}/Mg m^{-3}	2.051	1.634	2.000
μ/mm^{-1}	6.220	5.260	4.426
Reflections (total, independent, R_{int})	11953, 4571, 0.0376	16986, 6118, 0.0640	28948, 10353, 0.0428
Data/restraints/parameters	4571, 0, 271	6118, 0, 337	10353, 0, 622
Final $R1$, $wR2$ indices[b]	0.0334, 0.0949	0.0394, 0.0702	0.0342, 0.0782

[a] All measurements were made on a Bruker SMART diffractometer using Mo-Kα radiation. [b] $R1$ value is based on selected data [with $I > 2\sigma(I)$]; $wR2$ value is based on all data.

The compound $[Re(CO)_3Cl(dpq)][Gd(hfac)_3(H_2O)_2]\cdot C_6H_6$ was prepared in exactly the same way as **Re-Gd′**, by slow evaporation of a 1 : 1 mixture of $[Re(CO)_3Cl(dpq)]$ and $[Gd(hfac)_3(H_2O)_2]$ in CH_2Cl_2/benzene solution. Orange crystals were isolated in which it was shown that the $\{Gd(hfac)_3\}$ unit was not bound to the $[Re(CO)_3Cl(dpq)]$ fragment (see main text). Anal. Calcd. for: $C_{45}H_{28}N_4ClF_{18}GdO_{11}Re$: C, 35.5; H, 1.9; N, 3.7. Found: C, 35.5; H, 1.6; N, 4.1% (*NB*: This assumes 1.5 C_6H_6 of crystallisation. Only one C_6H_6 molecule was explicitly located in the crystal structure but an area of badly disordered solvent was also present which could not be modelled).

X-Ray crystallography

For each complex a suitable crystal was coated with hydrocarbon oil and attached to the tip of a glass fibre, which was then transferred to a Bruker-AXS SMART diffractometer under a stream of cold N_2. Details of the crystal parameters, data collection and refinement for each of the structures are collected in Table 6. After data collection, in each case an empirical absorption correction (SADABS) was applied,[15] and the structures were then solved by conventional direct methods and refined on all F^2 data using the SHELX suite of programs.[16] In all cases, non-hydrogen atoms were refined with anisotropic thermal parameters, hydrogen atoms were included in calculated positions and refined with isotropic thermal parameters which were *ca.* 1.2 × (aromatic CH) or 1.5 × (Me) the equivalent isotropic thermal parameters of their parent carbon atoms. The only significant problems were associated with the structural determination of $[Re(CO)_3Cl(dpq)][Gd(hfac)_3(H_2O)_2]\cdot C_6H_6$ for which the crystals scattered relatively weakly and only data with $2\theta \leq 50°$ was used in the final refinement. For the $[Gd(hfac)_3(H_2O)_2]$ fragment, 12 of the 18 fluorine atoms and five of the carbon atoms [C(113), C(114), C(116), C(117), C(127)] needed to be refined with isotropic thermal parameters to keep the refinement stable, geometric restraints were applied to some of the C–C distances in one of the hfac ligands, and those six F atoms that were refined with anisotropic displacement parameters required strong isotropic restraints. An area of diffuse, disordered electron density that could not be satisfactorily modelled was eliminated using the SQUEEZE command in PLATON. There is a large residual electron density peak of ≈ 5 e Å^{-3} located close (0.8 Å) to the Gd atom.

CCDC reference numbers 626876–626879.

For crystallographic data in CIF or other electronic format see DOI: 10.1039/b616423d

Acknowledgements

We thank the EPSRC for financial support.

References

1 (*a*) D. Imbert, M. Cantuel, J.-C. G. Bünzli, G. Bernardinelli and C. Piguet, *J. Am. Chem. Soc.*, 2003, **125**, 15698; (*b*) S. Torelli, D. Imbert, M. Cantuel, G. Bernardinelli, S. Delahaye, A. Hauser, J.-C. G. Bünzli and C. Piguet, *Chem.–Eur. J.*, 2005, **11**, 3228; (*c*) S. I. Klink, H. Keizer and F. C. J. M. van Veggel, *Angew. Chem., Int. Ed.*, 2000, **39**, 4319; (*d*) S. J. A. Pope, B. J. Coe and S. Faulkner, *Chem. Commun.*, 2004, 1551; (*e*) S. J. A. Pope, B. J. Coe, S. Faulkner and R. H. Laye, *Dalton Trans.*, 2005, 1482; (*f*) S. J. A. Pope, B. J. Coe, S. Faulkner, E. V. Bichenkova, X. Yu and K. T. Douglas, *J. Am. Chem. Soc.*, 2004, **126**, 9490; (*g*) S. J. A. Pope, B. P. Burton-Pye, R. Berridge, T. Khan, P. J. Skabara and S. Faulkner, *Dalton Trans.*, 2006, 2907; (*h*) P. D. Beer, F. Szemes, P. Passaniti and M. Maestri, *Inorg. Chem.*, 2004, **43**, 3965; (*i*) P. B. Glover, P. R. Ashton, L. J. Childs, A. Rodger, M. Kercher, R. M. Williams, L. De Cola and Z. Pikramenou, *J. Am. Chem. Soc.*, 2003, **125**, 9918; (*j*) D. Guo, C. Duan, F. Lu, Y. Hasegawa, Q. Meng and S. Yanagida, *Chem. Commun.*, 2004, 1486; (*k*) H.-B. Xu, L.-X. Shi, E. Ma, L.-Y. Zhang, Q.-H. Wei and Z.-N. Chen, *Chem. Commun.*, 2006, 1601; (*l*) J. W. Stouwdam, M. Raudsepp and F. C. J. M. van Veggel, *Langmuir*, 2005, **21**, 7003.

2 (*a*) T. A. Miller, J. C. Jeffery, M. D. Ward, H. Adams, S. J. A. Pope and S. Faulkner, *Dalton Trans.*, 2004, 1524; (*b*) G. M. Davies, S. J. A. Pope, H. Adams, S. Faulkner and M. D. Ward, *Inorg. Chem.*, 2005, **44**, 4656; (*c*) J.-M. Herrera, S. J. A. Pope, H. Adams, S. Faulkner and M. D. Ward, *Inorg. Chem.*, 2006, **45**, 3895; (*d*) J.-M. Herrera, M. D. Ward, H. Adams, S. J. A. Pope and S. Faulkner, *Chem. Commun.*, 2006, 1851; (*e*) S. G. Baca, H. Adams and M. D. Ward, *CrystEngComm*, 2006, **8**(8), 635.

3 (*a*) N. M. Shavaleev, L. P. Moorcraft, S. J. A. Pope, Z. R. Bell, S. Faulkner and M. D. Ward, *Chem. Commun.*, 2003, 1134; (*b*) N. M. Shavaleev, L. P. Moorcraft, S. J. A. Pope, Z. R. Bell, S. Faulkner and

M. D. Ward, *Chem.–Eur. J.*, 2003, **9**, 5283; (*c*) N. M. Shavaleev, G. Accorsi, D. Virgili, Z. R. Bell, T. Lazarides, G. Calogero, N. Armaroli and M. D. Ward, *Inorg. Chem.*, 2005, **44**, 61; (*d*) T. K. Ronson, T. Lazarides, H. Adams, S. J. A. Pope, D. Sykes, S. Faulkner, S. J. Coles, M. B. Hursthouse, W. Clegg, R. W. Harrington and M. D. Ward, *Chem.–Eur. J.*, 2006, **12**, 9299.
4 (*a*) R. Ruminski and R. T. Cambron, *Inorg. Chem.*, 1990, **29**, 1575; (*b*) J. R. Kirchhoff and K. Kirschbaum, *Polyhedron*, 1998, **17**, 4033; (*c*) J. A. Baiano and W. R. Murphy, *Inorg. Chem.*, 1991, **30**, 4594.
5 (*a*) S. L. James, M. Younus, P. R. Raithby and J. Lewis, *J. Organomet. Chem.*, 1997, **542**, 233; (*b*) M. Hissler, M. Connick, D. K. Geiger, J. E. McGarrah, D. Lipa, R. J. Lachiotte and R. Eisenberg, *Inorg. Chem.*, 2000, **39**, 447; (*c*) E. C. Whittle, J. A. Weinstein, M. W. George and K. S. Schanze, *Inorg. Chem.*, 2001, **40**, 4053; (*d*) S.-C. Chan, M. C. W. Chan, Y. Wang, C.-M. Che, K.-K. Cheung and N. Zhu, *Chem.–Eur. J.*, 2001, **7**, 4180; (*e*) F. Hua, S. Kinayyigit, J. R. Cable and F. N. Castellano, *Inorg. Chem.*, 2005, **44**, 471; (*f*) E. O. Danilov, I. E. Pomestchenko, S. Kinayyigit, P. L. Gentili, M. Hissler, R. Ziessel and F. N. Castellano, *J. Phys. Chem.*, 2005, **109**, 2465; (*g*) L. Zhang, Y.-H. Niu, A. K.-Y. Jen and W. Lin, *Chem. Commun.*, 2005, 1002.
6 Y.-Y. Ng, C.-M. Che and S.-M. Peng, *New J. Chem.*, 1996, **20**, 781.
7 N. M. Shavaleev, Z. R. Bell and M. D. Ward, *J. Chem. Soc., Dalton Trans.*, 2002, 3925.
8 J. A. Baiano, D. L. Carlson, G. M. Wolosh, D. E. Dejesus, C. F. Knowles, E. G. Szabo and W. R. Murphy, *Inorg. Chem.*, 1990, **29**, 2327.
9 (*a*) R. Engelman and J. Jortner, *Mol. Phys.*, 1970, **18**, 145; (*b*) W. Siebrand, *J. Chem. Phys.*, 1967, **47**, 2411; (*c*) S. D. Cummings and R. Eisenberg, *J. Am. Chem. Soc.*, 1996, **118**, 1949.
10 (*a*) D. Parker and J. A. G. Williams, Responsive luminescent lanthanide complexes, in *Metal Ions in Biological Systems*, vol. 40, ed. A. Sigel and H. Sigel, Marcel Dekker, New York, 2003; (*b*) N. Sabbatini, M. Guardigli and J.-M. Lehn, *Coord. Chem. Rev.*, 1993, **123**, 201.
11 M. R. Waterland, T. J. Simpson, K. C. Gordon and A. K. Burrell, *J. Chem. Soc., Dalton Trans.*, 1998, 185.
12 (*a*) M. F. Richardson, W. F. Wagner and D. E. Sands, *J. Inorg. Nucl. Chem.*, 1968, **30**, 1275; (*b*) Y. Hasegawa, Y. Kimura, K. Murakoshi, Y. Wada, J. Kim, N. Nakashima, T. Yamanaka and S. Yanagida, *J. Phys. Chem.*, 1996, **100**, 10201.
13 N. M. Shavaleev, S. J. A. Pope, Z. R. Bell, S. Faulkner and M. D. Ward, *Dalton Trans.*, 2003, 808.
14 (*a*) A. P. Bisson, C. A. Hunter, J. C. Morales and K. Young, *Chem.–Eur. J.*, 1998, **4**, 845; (*b*) The program is available for free download from: http://www.chris-hunter.staff.shef.ac.uk/soft.html.
15 G. M. Sheldrick, *SADABS, A program for absorption correction with the Siemens SMART area-detector system*, University of Göttingen: 1996.
16 G. M. Sheldrick, *SHELXS-97 and SHELXL-97 programs for crystal structure solution and refinement*, University of Göttingen, 1997.